1 *Xanthomonas* infection transforms the apoplast into an accessible and habitable niche for

2 *Salmonella enterica*

3

4 Megan H. Dixon[a,b], Kimberly N. Cowles[a], Sonia C. Zaacks[a], Isabel N. Marciniak[a], and Jeri D.

5 Barak[a*]

6

7 [a]Department of Plant Pathology, University of Wisconsin, Madison, Wisconsin, USA;

8 [b]Microbiology Doctoral Training Program, University of Wisconsin, Madison, Wisconsin, USA

9

10 Running Head: Water-Soaking Protects *Salmonella enterica*

11

12 Address correspondence to Jeri D. Barak, jeri.barak@wisc.edu

13

14 Abstract word count: 215 (143 for *Importance* section)

15 Text word count: 4,863 (excluding Materials and Methods, References, Tables, and Figure

16 Legends)

ABSTRACT

The physiology of plant hosts can be dramatically altered by phytopathogens. *Xanthomonas hortorum* pv. *gardneri* is one such pathogen that creates an aqueous niche within the leaf apoplast by manipulating the plant via the transcription activator-like effector AvrHah1. Simultaneous immigration of *X. gardneri* and *Salmonella enterica* to healthy tomato leaves results in increased survival of *S. enterica* as *Xanthomonas* infection progresses. However, the fate of *S. enterica* following arrival on actively infected leaves has not been examined. We hypothesized that the water-soaking caused by *X. gardneri* could facilitate the ingression of *S. enterica* into the apoplast, and that this environment would be conducive for growth. We found that a water-soaked apoplast, abiotically or *Xanthomonas*-infected, enabled surface *S. enterica* to passively localize to the protective apoplast and facilitated migration of *S. enterica* to distal sites within the aqueous apoplast. *AvrHah1* contributed to the protection and migration of *S. enterica* early in *X. gardneri* infection. *Xanthomonas*-infected apoplasts facilitated prolonged survival and promoted *S. enterica* replication compared to healthy apoplasts. Access to an aqueous apoplast in general protects *S. enterica* from immediate exposure to irradiation whereas, the altered environment created by *Xanthomonas* infection provides growth-conducive conditions for *S. enterica*. Overall, we have characterized an ecological relationship in which host infection converts an unreachable niche to a habitable environment.

Importance: Bacterial spot disease caused by *Xanthomonas* species devastates tomato production worldwide. Salmonellosis outbreaks from consumption of raw produce have been linked to the arrival of *Salmonella enterica* on crop plants in the field via contaminated irrigation water. Considering that *Xanthomonas* is difficult to eradicate, it is highly likely that *S. enterica*

40 arrives on leaves pre-colonized by *Xanthomonas* with infection underway. Our study
41 demonstrates that infection and disease fundamentally alter the leaf, resulting in redistribution
42 and change in abundance of a phyllosphere bacterial member. These findings contribute to our
43 understanding of how *S. enterica* manages to persist on leaf tissue despite lacking the ability to
44 liberate nutrients from plant cells. More broadly, this study reveals a mechanism by which
45 physiochemical changes to a host environment imposed by a plant pathogen can convert an
46 uninhabitable leaf environment into a hospitable niche for select epiphytic microbes.

47 **INTRODUCTION**

48 Within an environment as dynamic and complex as the phyllosphere, water is one of the
49 most critical factors for microorganism survival (1). The waxy cuticle limits the amount of
50 moisture available to bacteria that colonize leaves. However, surface bacteria have been known
51 to colonize particularly leaky areas of the cuticle such as leaf veins, cell junctions, and the base
52 of glandular trichomes (2–4). Some phytopathogenic bacteria have adapted to the water scarcity
53 issue by creating their own aqueous environment within the apoplast of leaf tissues (5–7).
54 Infection relies on first entering the leaf through stomata and then colonizing the extracellular
55 internal space, or apoplast, within the leaf. *Xanthomonas hortorum* pv. *gardneri* (hereafter, *X.*
56 *gardneri*), a causal agent of bacterial spot disease of tomato and pepper, is one such plant
57 pathogen that infects leaves. Once *X. gardneri* has actively migrated to the apoplast, it can
58 deploy its type-III secretion system to manipulate the host into leaking cellular constituents into
59 this space (6), creating an aqueous environment. These physiochemical modifications greatly
60 benefit *X. gardneri* but devastate its host. Bacterial spot disease often results in necrotic lesions
61 on leaves and fruit and defoliation (8) which are detrimental to the health of the plant.

62 Diseased plants are hosts to a diverse community of microbes, which can be influenced
63 by the drastic changes to their environment caused by phytopathogen infection (9–11). Microbes
64 that are non-pathogenic to plants can benefit from disease. For example, enteric human
65 pathogens such as *Salmonella enterica* lack enzymes that would enable the liberation of nutrients
66 directly from plant cells (12, 13) and are typically forced to scavenge scant resources on the leaf
67 surface. On healthy plant tissues, *S. enterica* populations decline over time (14, 15). However,
68 plant pathogens and even insect pests that exist in agricultural fields have been shown to enhance
69 *S. enterica* populations on plant leaves, and such organisms that can promote *S. enterica*

70 persistence and/or replication have been coined "biomultipliers" (15–19). Bacterial pathogens
71 including *Xanthomonas* spp. and *Pectobacterium carotovorum* have been implicated as
72 biomultipliers for *S. enterica* on leaves (15–17, 20, 21). The mechanisms explaining how these
73 organisms benefit *S. enterica* are not well understood, posing ecological questions with
74 important agricultural and human disease epidemiological implications.

75 The prevalence of food-borne illness outbreaks linked to consumption of raw produce has
76 climbed in the past few decades (22). Such outbreaks have been linked to pre-harvest
77 contamination of crops in the field via irrigation water (23, 24). The presence of enteric
78 pathogens within internal plant tissues has been a concern of food safety researchers, especially
79 considering efforts to mitigate outbreaks through post-harvest sanitation of produce. Various
80 studies investigated *S. enterica* colonization of the leaf apoplast, and the extent to which *S.*
81 *enterica* can colonize this protective niche varies based on host and method. The flagella-
82 dependent localization of *S. enterica* to internal tissue in response to light has been demonstrated
83 via confocal microscopy of lettuce leaf pieces submerged in *S. enterica* inoculum (25). However,
84 tomato leaves have been shown to be impermeable to *S. enterica* internalization when compared
85 with lettuce leaves under comparable conditions (26, 27). Whether or not phytopathogen
86 infection could enhance the permeability of leaves to enteric pathogens was not addressed by
87 these studies.

88 *Xanthomonas* infection promotes *S. enterica* survival when both the plant and human
89 pathogen arrive on healthy tomato leaves simultaneously (15, 16, 21), however, the fate of *S.*
90 *enterica* on leaves actively infected with *Xanthomonas* spp. has not been described. *X. gardneri*
91 infection can facilitate the migration of surface *X. gardneri* cells to distal tissue via absorption of
92 *X. gardneri* suspensions into needle-damaged tissue (6), suggesting that water-soaking may

93 promote the ingression of bacteria into the apoplast of leaves when external water is present.
94 Water-soaking has been demonstrated to be enhanced by *X. gardneri* type-III effector AvrHah1
95 (6, 28). *AvrHah1* encodes a transcription activator-like effector that binds host DNA and
96 upregulates the activity of a host pectate lyase (6), forcing the host to degrade the pectin
97 "cement" that joins adjacent plant cells, resulting in an aqueous apoplast (29). Data from our lab
98 has shown that *avrHah1* expression by *X. gardneri* is necessary for enhancing the persistence of
99 *S. enterica* on tomato leaves when co-inoculated with *X. gardneri* (21). Based on these
100 observations, we hypothesized that *avrHah1*-dependent water-soaking and aqueous apoplasts in
101 general could serve as a mechanism for epiphytic *S. enterica* to enter protected sites of leaves.
102 The goal of our study was to examine the fate of epiphytic *S. enterica* following arrival
103 on the surface of infected leaves. We examined whether an abiotically water-soaked or
104 *Xanthomonas*-infected apoplast could facilitate the relocation of *S. enterica* to protected niches,
105 particularly in the absence of leaf wounding. *S. enterica* populations were considered protected if
106 they survived UV irradiation applied to leaves. We also identified the roles of *avrHah1*,
107 *Xanthomonas* infection progress, and *S. enterica* motility on *S. enterica* entry into the apoplast
108 and subsequent migration beyond the arrival site. Lastly, we investigated whether the aqueous
109 niche created by *Xanthomonas* species enhanced the prolonged survival of *S. enterica* within the
110 apoplast to determine whether factors aside from water availability contribute to *S. enterica*
111 survival in the apoplast. Identifying host and microbial factors that influence the redistribution
112 and survival of a model epiphyte will broaden our understanding of microbe-facilitated
113 adaptations by plant-associated bacteria.

114 **METHODS**

115 **Bacterial Strains, Media, and Culture Conditions**

116 Bacterial strains used in this study are described in Table 1. *Xanthomonas* cultures were prepared
117 by inoculating nutrient broth (NB) with frozen cells and incubating at 28°C with shaking at 200
118 rpm for two days. *S. enterica* cultures were prepared similarly but grown in lysogeny broth (LB)
119 and incubated overnight. Cultures were prepared to desired cell concentrations via dilution in
120 sterile water as described below.

121

122 **Plant Infiltration**

123 For all experiments, *Solanum lycopersicum* (tomato) cultivar Moneymaker seedlings were
124 cultivated in growth chambers with a 16 hr photoperiod at 24°C. For *Xanthomonas* infiltration
125 experiments, 5-week-old tomato plants were infiltrated with *Xanthomonas* and inoculated with
126 droplets of *S. enterica* as described previously (6) with modifications (Fig. 1). *Xanthomonas*
127 cultures were prepared to an optical density at 600 nm (OD_{600}) = 0.3, 0.25, or 0.2 (10^8 CFU/mL)
128 for *X. gardneri* WT, *X. gardneri avrHah1*$^{\Delta DBD}$, and *X. vesicatoria*, respectively, and infiltrated
129 into two leaflets per plant on the third true leaf via needleless syringe. Infiltration medium was
130 gently forced into the leaf tissue through the abaxial leaf surface until the infiltration zone was
131 approximately 2 cm long, and then the infiltration zone was outlined with permanent marker.
132 When applicable, a subset of plants was infiltrated with sterile water as a control. When *S.*
133 *enterica* infiltration was utilized as a control for one experiment, similar methods were applied,
134 although the *S. enterica* culture used for infiltration was prepared to a concentration of 10^7
135 CFU/mL and infiltrations were performed in a biosafety cabinet.

136 Following infiltration, plants were then incubated in bins with lids on at a relative
137 humidity (RH) > 90% for 1-2 days prior to subsequent *S. enterica* application. For some
138 experiments, infiltration with sterile water was delayed for a subset of plants until immediately
139 prior to *S. enterica* inoculation to simulate arrival of *S. enterica* on healthy water-soaked tissue.
140 These plants were incubated alongside the already infiltrated plants prior to their infiltration such
141 that environmental conditions would be consistent among all plants within an experiment.
142
143 **Droplet Inoculation**
144 Lids of plant bins were removed to inoculate leaflets with *S.* enterica, effectively reducing the
145 RH to ~70%. Infiltrated leaflets were marked again with permanent marker on the *S. enterica*
146 arrival day to designate the site of *S. enterica* droplet placement on the infiltration zone. *S.*
147 *enterica* cultures were prepared to an OD_{600}= 0.1 (10^8 CFU/mL) and 15 µL droplets of the
148 normalized *S. enterica* culture were applied to the adaxial surface within the part of the
149 infiltration zone closest to the leaf margin. For one experiment in which *S. enterica* was applied
150 at a lower inoculation level, the normalized culture was diluted 1000-fold prior to inoculation.
151 Note that droplets were applied such that they did not overlap with any minor tissue damage
152 caused by the needleless syringe infiltration from the abaxial surface. Plants inoculated with *S.*
153 *enterica* remained inside plastic bins, and the lids were kept off (RH ~70%) until droplets were
154 no longer visible (i.e., absorbed or evaporated). Visual observations of droplet absorption
155 (complete, partial, or none) were recorded at 2.5 hours after droplet application. When specified,
156 a micropipette was used for removing each remaining droplet and measuring their volume. Leaf
157 tissue was then sampled destructively at the indicated time post-*S. enterica* arrival to quantify

158 bacterial populations. For experiments requiring sampling beyond 2.5 hours post-*S. enterica*
159 arrival, bins lids were replaced to maintain plants at >90% RH until sampling.
160
161 **Bacterial Population Sampling**
162 Whole leaflets were removed at the petiolule and when specified, treated with 254 nm UV
163 radiation (Stratalinker® UV Crosslinker 1800) at 600,000 μJ/cm^2 with the adaxial leaf surface
164 facing upwards towards the bulb in order to inactivate surface *S. enterica* cells and enrich for
165 apoplastic *S. enterica*. The effect of 600,000 μJ/cm^2 of UV irradiation on surface *S. enterica*
166 populations was determined by removing surface *S. enterica* cells 1 day post-droplet inoculation
167 using a cotton swab dipped in 0.1% Tween-20 and gently wiping it across the adaxial surface of
168 the leaf for 5 seconds. The tip of the cotton swab was vortexed in 500 uL of water for 5 seconds,
169 and then the cell mixture was dilution-plated to enumerate surface *S. enterica* populations (Fig.
170 S1).
171 Leaflets irradiated with UV were chosen at random between the two leaflets sampled per
172 plant and the second leaflet was left non-irradiated as a control. Bacterial populations were
173 measured as described previously (18). Unless noted otherwise, all inoculated leaflets were
174 sampled regardless of observations made at the droplet absorption stage. Briefly, leaf tissue was
175 excised using a sterile 1 cm diameter tissue corer and homogenized in 500 μL of sterile water
176 using a hand Dremel. For *S. enterica* droplet-inoculated tissue, the site of *S. enterica* arrival was
177 sampled by centering the tissue corer between the marker guidelines. When indicated, tissue was
178 also sampled distal from the arrival site by excising a second tissue core 1-2 mm away from the
179 first leaf disk overlapping the infiltration zone. Leaf tissue homogenate was dilution-plated on
180 LB agar amended with 50 μg/mL kanamycin for enumeration of *S. enterica* populations. When

181 *S. enterica* was applied at a low dosage, the leaf tissue homogenate that remained after plating
182 was enriched with LB amended with kanamycin (50 ug/mL) to determine if *S. enterica* was
183 present, but below the limit of detection for dilution-plating. LB-enriched samples were plated
184 22-24 hours later. *S. enterica* colonies were enumerated after 1 day of incubation at 37°C.
185
186 **Statistical Analyses**
187 R Studio version 2021.09.1 (R Development Core Team, R Foundation for Statistical
188 Computing, Vienna, Austria [http://www.R-project.org]) was utilized for all statistical analyses
189 and plot generation. Each experiment was repeated three times, and each boxplot represents the
190 aggregation of three independent experiments found to be statistically similar ($P > 0.05$), unless
191 noted otherwise in the figure legend. Within each experiment, the number of biological replicates
192 N = 4-8 leaflets. For comparing *S. enterica* populations among treatment groups at the arrival
193 tissue site, the ANOVA and post-hoc Tukey tests were used. When two leaflets were inoculated
194 per plant, the data were fit to a linear mixed effects model using the lme4 package in which
195 individual plants were modeled as a random effect. *S. enterica* population data at distal tissue
196 sites were generally not found to be normally distributed due to zeroes resulting from the
197 absence of *S. enterica* migration beyond the initial site of arrival. Therefore, for comparing *S.*
198 *enterica* populations among treatment groups at the distal tissue site, the non-parametric
199 Kruskal-Wallis and post-hoc Wilcox tests were used. In addition, the proportion of samples with
200 detectable bacterial populations at the distal tissue site were compared using the Fisher's Exact
201 Test to compare the incidence of *S. enterica* colonization of distal tissue. For the low *S. enterica*
202 dosage experiment, data from the healthy/dry treatment was excluded from the mixed effects
203 model because the value of nearly every data point was zero. Preliminary analysis indicated that

204 for the remaining two treatments (healthy/wet and *X.* gardneri-infected), all means were greater
205 than zero based on one-way t-tests ($P < 0.05$). When applicable, the limit of detection minus one
206 (i.e., 49 CFU/leaf disk) was substituted for non-detects. The significance threshold for all
207 comparisons was $P < 0.05$.
208
209 **RESULTS**
210 **Abiotically water-soaked apoplasts enable *S. enterica* to migrate via stomata to a**
211 **UV-protected niche.** To characterize the role of water in the apoplast in the migration of *S.*
212 *enterica* to a protected niche and migration to sites distal to the arrival site, we developed a
213 method involving infiltration of intact tomato leaflets, application of droplets of *S. enterica* cell
214 suspensions, and measurement of UV-protected *S. enterica* populations (Fig. 1). Our methods
215 were inspired by work previously published by Schwartz et al. (6), with a few key differences
216 that included applying bacterial droplets to intact (not detached) leaflets onto the adaxial surface,
217 refraining from wounding the leaves at the droplet application site, and utilizing UV irradiation
218 to enrich for apoplastic *S. enterica* populations. We found that our UV irradiation methods
219 reduced the *S. enterica* populations on the leaf surface by 2.9 logs (Fig. S1). Additionally, we
220 manipulated the timing of *S. enterica* arrival on water-infiltrated leaves to observe how the
221 presence of water in the apoplast influences the relocation of *S. enterica*.
222 Infiltration of water into the apoplast simulated abiotic water-soaking that may occur
223 during periods of high precipitation (30). Under the tested conditions (~70% RH), water
224 infiltration created an obvious darkening or "wet" appearance to the tissue that lasted for a few
225 hours (data not shown). *S. enterica* droplets were applied to two treatments: leaves with a (i)
226 "healthy/dry" apoplast where the tissue had become macroscopically dry at time of *S. enterica*

227 application at 2 day post-infiltration (DPI) or (ii) "healthy/wet" apoplast where tissue was still
228 visibly dark and wet in appearance when *S. enterica* was applied within 10 minutes of water
229 infiltration (0 DPI). A third treatment was included in which we infiltrated *S. enterica* directly
230 into the apoplast to determine the relative amount of UV protection provided to apoplastic *S.*
231 *enterica* cells.

232 Within a few hours of *S. enterica* arrival on the leaf, we observed the disappearance of
233 the droplets specifically into healthy/wet tissue in the absence of any applied epidermal
234 wounding, suggesting that the *S. enterica* suspension had been absorbed through stomata.
235 Leaflets were observed for a duration of 2.5 hours post-application of *S. enterica,* and absorption
236 of the entire 15 μL suspension could be observed within a minimum of 30 minutes. The success
237 rate for complete absorption of the droplet for healthy/wet tissue varied between 50-83% among
238 three experimental replicates, although droplets that failed to be completely absorbed within the
239 2.5 hour timeframe had visibly reduced in size, suggesting that they were partially absorbed. By
240 contrast, healthy/dry leaflets had an absorption rate of 0%. Beyond the observation period, after
241 several hours had passed, all droplets disappeared either by absorption, evaporation, or both. *S.*
242 *enterica* populations were enumerated at 1 day post-arrival, and among the three treatments, UV
243 irradiation resulted in the lowest *S. enterica* populations when *S. enterica* was applied to leaflets
244 with a healthy/dry apoplast (Fig. 2). These surface-limited populations were reduced ~2.5 logs
245 by UV irradiation. Arrival on healthy/wet tissue and direct infiltration into the apoplast resulted
246 in equivalent UV-protected populations and relatively small population reductions of ~0.9 and
247 ~0.7 logs, respectively, in response to UV irradiation (Fig. 2). The increased UV protection
248 conferred to *S. enterica* when applied to healthy water-soaked tissue suggests that an aqueous
249 apoplast provides a gateway for surface bacteria to move inside the leaf.

250 Next, we investigated whether movement of surface bacteria to the apoplast was limited
251 to the immediate substomatal chamber or extended beyond. We observed distinct differences in
252 the ability of *S. enterica* to migrate from the arrival site to tissue non-overlapping the droplet
253 application site depending on the physical state of the apoplast. A healthy/dry apoplast did not
254 readily facilitate lateral migration of *S. enterica* to areas within the apoplast distal from the
255 arrival site whereas, a healthy/wet apoplast enabled recovery of significantly higher *S. enterica*
256 populations at distal sites (Fig. 2). Distal sites within the apoplast provided *S. enterica* with a
257 protected niche if the apoplast was an aqueous environment at time of *S. enterica* arrival, as the
258 population reduction in response to UV irradiation was only ~0.5 logs (Fig. 2). These findings
259 support the conclusion that an aqueous apoplast permits surface bacteria to migrate beyond the
260 initial arrival site.

261 ***Xanthomonas* water-soaking promotes *S. enterica* entry to the apoplast and**
262 **facilitates migration to distal tissue.** *X. gardneri* is known to cause water-soaking (6, 28), and
263 thus we examined whether *X. gardneri* infection could confer protection to *S. enterica* against
264 UV irradiation and facilitate its migration to infected sites distal from the initial site similarly to a
265 healthy/wet apoplast. We found that *X. gardneri*-infected tissue enabled complete absorption of
266 *S. enterica* droplets into the leaves at 1 DPI (Fig. S2) and 2 DPI (images not shown) within 0.5-
267 2.5 hours. To assess the protection of absorbed *S. enterica* cells against UV, we infiltrated an
268 excess number of plants with *X. gardneri*, and the first 50% of plants that completely absorbed
269 the droplets were specifically selected for *S. enterica* population sampling at 1 day post-*S.*
270 *enterica* arrival. *S. enterica* cells were found to be more protected against UV irradiation
271 following droplet absorption into *X. gardneri*-infected tissue at 2 DPI compared to *S. enterica*
272 cells that were limited to the surface of healthy/dry tissue (Fig. 3). Like a healthy/wet apoplast, a

273 *X. gardneri*-infected apoplast facilitated robust colonization of *S. enterica* cells to sites in the
274 apoplast beyond the initial arrival site, where *S. enterica* was protected from UV irradiation (Fig.
275 3b).

276 ***AvrHah1* facilitates *S. enterica* localization to the apoplast and lateral migration**
277 **early in infection**. Knowing that an aqueous apoplast facilitates the migration of *S. enterica* to a
278 protected niche within a day of arrival, we examined whether protection against UV irradiation
279 exists as early as 2.5 hours post-arrival, a time point at which *S. enterica* droplet suspensions
280 were often completely absorbed. Also, we compared the fate of *S. enterica* following arrival on
281 tissue infected by one of three *Xanthomonas* strains including *X. gardneri* WT, *X. gardneri*
282 *avrHah1*$^{\Delta DBD}$, and *X. vesicatoria*. *X. vesicatoria* is a pathogen within the bacterial spot disease
283 complex that lacks *avrHah1* and has been shown in co-inoculation experiments with *S. enterica*
284 to not promote *S. enterica* growth on tomato leaves, in contrast to *X. gardneri,* which does
285 facilitate *S. enterica* replication (15, 21).

286 The duration of infection with *Xanthomonas* spp. was found to affect visible water-
287 soaking, absorption of the *S. enterica* suspension, and *S. enterica* protection from UV irradiation
288 (Fig. 4). Tissue infected with *Xanthomonas* spp. was generally water-soaked at 1 and 2 DPI,
289 except for leaflets infected with the *X. gardneri avrHah1*$^{\Delta DBD}$ strain at 1 DPI (Fig. S3). Leaflets
290 infected with *X. vesicatoria* became water-soaked at a similar rate as *X. gardneri* WT-infected
291 leaflets despite lacking the *avrHah1* gene. As for effects on *S. enterica*, tissue that was
292 macroscopically dry at *S. enterica* arrival, which included the healthy/dry and *X. gardneri*
293 *avrHah1*$^{\Delta DBD}$ 1 DPI treatments, did not absorb the *S. enterica* suspension, resulting in the highest
294 droplet recovery volumes at 2.5 hours post *S. enterica* droplet application (Fig. 4a). In contrast to
295 dry tissue, the recovered droplet volumes were lower for water-soaked tissue with healthy/wet,

296 *X. gardneri* WT-infected, or *X. vesicatoria*-infected leaves, and these tissues often absorbed the
297 *S. enterica* suspension completely (Fig. 4a). Congruently, *S. enterica* arrival on water-soaked
298 tissues resulted in the greatest protection, as evident by smaller reductions in population in
299 response to UV (Fig. 4b). Overall, infection progress had a significant effect on *S. enterica*
300 protection in our model.

301 In addition to facilitating initial entry of *S. enterica* into the substomatal chamber,
302 *avrHah1* was also found to contribute to the ability of *S. enterica* to migrate to distal tissue
303 beyond the site of arrival early in infection (Fig. 5). Leaves infiltrated with *X. gardneri*
304 *avrHah1*$^{\Delta DBD}$, which generally had a dry apoplast at 1 DPI (Fig. S3) and did not result in visible
305 absorption of the *S. enterica* suspension (Fig. 4a), exhibited reduced migration of *S. enterica* to
306 distal tissue compared to leaves infiltrated with *X. gardneri* WT (Fig. 5). However, by 2 DPI,
307 when the tissue was visibly water-soaked (Fig. S3), *X. gardneri avrHah1*$^{\Delta DBD}$-infected tissue did
308 facilitate colonization of distal tissue by *S. enterica* (Fig. 5). These findings demonstrate that the
309 role of *avrHah1* in altering the apoplast into an aqueous environment occurs early in the disease
310 progress, and these changes facilitate surface bacteria entry into the apoplast and subsequent
311 lateral migration to other water-soaked areas. We also note that additional bacterial factors
312 besides *avrHah1* contribute to water-soaking later in disease progression.

313 **Active motility of *S. enterica* increases colonization of tissue beyond the arrival site**
314 **as *X. gardneri* infection progresses.** To test the hypothesis that active *S. enterica* motility
315 contributes to migration away from the surface, bacterial populations for a *S. enterica* Δ*motA*
316 mutant with non-functional flagella were compared to a wild-type *S. enterica* strain. At 2.5 hours
317 post-*S. enterica* arrival, the Δ*motA* mutant colonized UV-protected sites of water-soaked leaves
318 equivalently to the wild-type *S. enterica* strain (Fig. S4), indicating that motility does not affect

319 *S. enterica's* ability to enter the aqueous apoplast. We also compared *S. enterica* WT and Δ*motA*
320 populations at tissue distal from the arrival site at 1 day post-*S. enterica* arrival. Motility did not
321 affect *S. enterica* colonization of distal tissue infected with *X. gardneri* when *S. enterica* arrived
322 at 1 DPI, however, at 2 DPI, *S. enterica* populations at distal sites were enhanced by motility
323 (Fig. 5). Deletion of *motA* did not eliminate *S. enterica* colonization of distal tissue nor affect the
324 proportion of distal sites with detectable *S. enterica* populations, indicating that motility was
325 useful but not required for lateral migration of *S. enterica*. Overall, motility was not required for
326 entry into the apoplast or migration beyond the initial arrival site, supporting a model of passive,
327 rather than active, *S. enterica* relocation within water-soaked tissue.

328 **Prolonged survival of *S. enterica* in a protected niche is increased by *Xanthomonas***
329 **infection.** Having established that aqueous apoplasts result in similar migration of *S. enterica* to
330 UV-protected niches regardless of whether the apoplast is abiotically water-soaked or water-
331 soaked via *Xanthomonas* infection, we then tested the hypothesis that the apoplast of
332 *Xanthomonas* infected leaves would support higher *S. enterica* population growth than healthy
333 leaves following *S. enterica* application at 1 DPI. We found that *S. enterica* arrival on *X.*
334 *gardneri* WT or *X. vesicatoria*-infected tissue resulted in the highest UV-protected *S. enterica*
335 populations at three days post-arrival (Fig. 6). Although a healthy/wet apoplast facilitated equal
336 colonization of *S. enterica* within UV-protected areas compared to *X. gardneri* WT and *X.*
337 *vesicatoria* infected tissue at 2.5 hours post-*S. enterica* arrival, (Fig. 4b) the healthy/wet apoplast
338 supported lower *S. enterica* populations at the arrival and distal sites relative to infected/wet
339 apoplasts by 3 days post-*S. enterica* arrival (Fig. 6). *X. gardneri avrHah1*$^{\Delta DBD}$-infected plants (1
340 DPI) did not permit droplet absorption (Table S1), yielded intermediate UV-protected *S. enterica*
341 populations at the arrival and distal sites (Fig. 6), and resulted in the most variable *S. enterica*

342 populations by 3 DPA (Fig. 6). Healthy/dry tissue also did not absorb the droplets (Table S1) and
343 supported the lowest *S. enterica* populations at the arrival and distal sites (Fig 6).
344 We also tested the hypothesis that *X. gardneri*-infected apoplasts support higher *S.*
345 *enterica* growth when *S. enterica* cells are applied to the leaves at a 1000 times lower inoculum
346 level (10^3 CFU/droplet) relative to the previous experiments. Reducing the *S. enterica* inoculum
347 dosage minimizes the possibility of overwhelming the plant immune response and more
348 realistically models foliar contamination of crops with *S. enterica*. Arrival of *S. enterica* on
349 healthy/dry leaves led to eradication of *S. enterica* populations in response to UV irradiation
350 (Fig. 7). Meanwhile, when *S. enterica* was applied to leaves with an aqueous apoplast (healthy or
351 *X. gardneri* WT-infected) it localized to UV-protected niches and migrated to distal tissue within
352 2.5 hours (Fig. 7). Additionally, the UV-protected populations increased between day 0 (2.5
353 HPA) and day 3 (3 DPA) (Fig. 7). *X. gardneri*-infected apoplasts supported the highest *S.*
354 *enterica* growth, resulting in *S. enterica* populations that increased at least 3.8 logs within 3 days
355 of arrival (Fig. 7). The higher apoplastic *S. enterica* populations observed in infected tissue
356 substantiates the conclusion that prolonged survival in the apoplast by surface bacteria is
357 supported by an aqueous environment resulting from phytobacterial infection, which is distinct
358 from a healthy, watery apoplast.
359
360 **DISCUSSION**
361 In this study, we determined the fate of *S. enterica* following arrival on *Xanthomonas*-
362 infected tissue, specifically regarding ingression into the apoplast and migration to distal sites.
363 We hypothesized that the modifications to the host caused by *Xanthomonas* infection could
364 facilitate ingression of *S. enterica* into the apoplast, where it could migrate to distal sites and

365 thrive. *S. enterica* was applied to leaves as a droplet to model splash dispersal of bacteria in the
366 field, which can occur during irrigation or precipitation events. Various host and microbial
367 factors including the presence of water in the apoplast, flagellar function by *S. enterica,* and
368 *avrHah1* expression by *X. gardneri* were manipulated to understand how alterations to the
369 infection court, the apoplast, impact plant-associated surface bacteria.

370 Colonization of protected niches such as the apoplast is essential to the lifestyle of
371 various plant-associated bacteria. To determine whether *S. enterica* could localize to protected
372 niches of leaves, UV irradiation at 254 nm, which is an FDA-approved method for
373 decontamination of food surfaces (31) and has been applied in previous plant bacterial endophyte
374 studies (32, 33), was utilized to reduce surface *S. enterica* populations. The use of UV irradiation
375 additionally models the UV exposure that plant-associated microbes are routinely exposed to,
376 though it's worth noting UV wavelengths less than 300 nm are typically absorbed by our
377 atmosphere and do not reach Earth (34). Initially, we tested whether *S. enterica* cells that were
378 infiltrated directly into the apoplast of leaves would be protected from UV irradiation applied to
379 the adaxial surface, and we hypothesized that the palisade cells, upper epidermal cells, and
380 cuticle would occlude UV penetration to the apoplastic *S. enterica*. We determined that *S.*
381 *enterica* cells localized to the apoplast were more protected from UV compared to *S. enterica* on
382 the surface, although UV irradiation reduced the apoplastic *S. enterica* populations a small but
383 statistically significant amount (Fig. 2). Leaves must permit light to penetrate leaf tissue for
384 photosynthesis and act as "light traps (35)," which may explain why a subset of apoplastic *S.*
385 *enterica* cells were vulnerable to UV. The duration of UV exposure influenced the magnitude of
386 *S. enterica* population reduction (data not shown), and the exposure level of 0.6 J/cm^2 selected
387 for these experiments resulted in >2.0 log reduction of surface *S. enterica* populations with

388 minimal effects on the apoplastic populations. As for the surface-localized *S. enterica* cells, the
389 small subpopulations that survived UV irradiation (Fig. S1) likely resisted sterilization by being
390 canopied by leaf surface structures, such as trichomes, or wedged within the grooves between
391 adjacent cells (36–38).

392 *S. enterica* successfully colonized UV-protected niches of abiotically water-soaked or
393 *Xanthomonas*-infected tissue. We rationalized that *S. enterica* had accessed the leaf apoplast
394 based on a few lines of evidence. First, the extent to which *S. enterica* was protected from UV
395 irradiation following arrival on abiotically water-soaked or *X. gardneri*-infected apoplast was
396 similar to cells infiltrated directly into the apoplast (Fig. 2). Second, *S. enterica* droplets were
397 absorbed by abiotically water-soaked or infected tissue, as evident by rapid disappearance of the
398 droplets in as little as 30 minutes. Healthy tissue is typically impermeable to spontaneous
399 absorption of surface water because the surface tension of water is greater than the critical
400 surface tension of the leaf surface (39). However, the relatively rapid disappearance of droplets
401 into water-soaked leaves indicated that the wettability of the leaf surface had changed.
402 Considering that the leaf tissue was deliberately not wounded, open stomata likely served as
403 entry points for external water and suspended *S. enterica* cells to enter the apoplast. We theorize
404 that an aqueous apoplast enabled a watery film to extend upwards through the stomatal pores,
405 providing a continuous "watery highway" that could facilitate movement of *S. enterica* into the
406 substomatal space. Lastly, *S. enterica* was consistently isolated at high levels from abiotically
407 water-soaked (Fig. 2) and infected (Fig. 3) tissue ~1 cm distal from the arrival site when the
408 apoplast was water-soaked at *S. enterica* arrival, but not when it was dry. Schwartz et al. found
409 that *X. gardneri*-infected leaves facilitated migration of surface *X. gardneri* cells to the apoplast
410 (6), and here we have confirmed that other bacteria besides the phytopathogen *X. gardneri* could

411 be transported by water-soaking. To verify that *S. enterica* colonization of distal tissue was not
412 driven by migration across the surface but by migration through the apoplast, the adaxial surface
413 of leaf tissue disks were pressed to agar plates following UV exposure. *S. enterica* was rarely
414 isolated from the surface of leaves distal to the arrival site with a healthy/dry apoplasts (data not
415 shown). Overall, *S. enterica* was found to relocate from the surface of leaves into the substomatal
416 chamber and beyond. These observations posed the question of whether *S. enterica* motility is
417 necessary for the redistribution of cells following *S. enterica* arrival.

418 Flagellar motility is key to survival on the leaf surface for recent immigrants (40), but we
419 found that the relocation of *S. enterica* from the leaf surface to the aqueous apoplast can occur
420 independent of functional flagella (Fig. 5), thus favoring a model of passive *S. enterica*
421 relocation in the presence of a water-soaked apoplast. However, active motility was found to
422 provide *S. enterica* with an advantage in colonizing sites beyond the initial arrive site at 2 days
423 post-*X. gardneri* infection, but not earlier (Fig. 5). *In planta* microscopy of *Pseudomonas*
424 *syringae* colonization has revealed that distinct bacterial subpopulations exist within infected
425 tissue, suggesting that the apoplast is a heterogeneous environment (41). Later in *Xanthomonas*
426 infection when more nutrients may be available in the apoplast, motile *S. enterica* cells may
427 employ chemotaxis to colonize nutritional micro-oases within the apoplast. Therefore, as the
428 *Xanthomonas* infection court dynamically changes over time, the importance of specific traits
429 possessed by plant-associated microbes also changes.

430 In addition to determining how *S. enterica* redistribution is affected by one of its own
431 genetic traits, we also examined the role of *X. gardneri* type-III effector AvrHah1 to identify
432 mechanisms by which phytopathogen infection influences the fate of *S. enterica. AvrHah1*
433 contributed to *S. enterica's* ability to access the protective apoplast (Fig. 4) and migrate to distal

434 tissue in the early stage of an ongoing *X. gardneri* infection (Fig. 5). AvrHah1 is the only
435 *Xanthomonas* effector that has been directly linked to the water-soaking phenotype, despite
436 water-soaking being a characteristic symptom of bacterial spot disease. Other Xanthomonads
437 outside of the bacterial spot complex that infect diverse hosts, including leafy greens, cause
438 water-soaking (42, 43), yet no other water-soaking effectors have been identified within the
439 *Xanthomonas* genus. Among the various *Xanthomonas* species that cause bacterial spot disease,
440 which includes *X. vesicatoria, X. euvesicatoria, and X. perforans, avrHah1* was originally
441 specific to *X. gardneri* (44, 45). Recently, however, *X. perforans* strains carrying *avrHah1* have
442 been identified in the southeastern United States (46). *X. vesicatoria,* which lacks *avrHah1,*
443 induced visible water-soaking of tomato leaves as rapidly as *X. gardneri* and promoted
444 protection and survival of *S. enterica* equal to or better than *X. gardneri.* These results contrast
445 with previous studies documenting that *X. vesicatoria* infection does not promote *S. enterica*
446 persistence on tomato leaf tissue following co-arrival of *X. vesicatoria* and *S. enterica* on healthy
447 plants (15, 21). However, a key difference between those studies and the study presented here is
448 the physiological state of the leaf when *S. enterica* arrives: healthy leaves versus infected leaves.
449 Infected tissue can permit *S. enterica* to enter the apoplast, and therefore, the benefits conferred
450 to *S. enterica* by *X. vesicatoria* infection may be conditional on *S. enterica* entry. Overall, the
451 ability of *avrHah1*-lacking *Xanthomonas* strains to facilitate water-soaking mediated ingression
452 of *S. enterica* into the apoplast and the observed delay, not elimination, of water-soaking in *X.*
453 *gardneri avrHah1*$^{\Delta DBD}$ suggest that other factors within the *Xanthomonas* genome independent
454 of *avrHah1* contribute to creating an aqueous niche within the tomato leaf apoplast. Identifying
455 these bacterial factors in future studies would improve our understanding of phytopathogen-
456 mediated water-soaking.

457 Leaf surfaces are harsh environments that require plant-associated bacteria to flexibly adapt to
458 extreme and dynamic conditions, including desiccation, heavy rainfall, UV irradiation, and
459 sporadic nutrient availability (47–50). Many phytopathogenic bacteria have evolved to infect the
460 apoplast of leaves where they can replicate to high population levels whilst exploiting host
461 resources (51). The apoplast can be protective and provide bacteria with increased nutrient
462 availability, however, this environment is exclusive to microbes that can successfully migrate
463 there and tolerate the host immune response. Tomato leaves are relatively restrictive to *S.*
464 *enterica* ingression (26, 27), yet we found that *S. enterica* can access an apoplast that is water-
465 soaked either by *Xanthomonas* infection or abiotically. Furthermore, *Xanthomonas* infection
466 resulted in higher *S. enterica* populations within UV-protected niches (Fig. 6) and enhanced *S.*
467 *enterica* replication (Fig. 7) relative to healthy leaf controls. *S. enterica's* capacity to exhibit near
468 4 log population growth within three days of *S. enterica's* arrival on the surface of *X. gardneri*-
469 infected leaves (Fig. 7) emphasizes the extent that *Xanthomonas* pathogens modify the apoplast.
470 An infected tomato leaf apoplast relieves suppression of *S. enterica* replication, suggesting that
471 *Xanthomonas* infection aids in overcoming the host immune response and/or liberates nutrients
472 inaccessible to *S. enterica*. *S. enterica* is known to elicit the plant immune response (52) upon
473 recognition of microbe-associated molecular markers such as flg22 (53, 54), although some
474 evidence suggests that the host response provoked by *S. enterica* is relatively weak (55, 56). If
475 modulation of the immune response by *Xanthomonas* does enhance *S. enterica* fitness in the
476 apoplast, it is likely that this is not the only mechanism involved. The replication of *S. enterica* in
477 an infected apoplast also suggests that nutrients have been made bioavailable by *Xanthomonas*
478 infection. *Xanthomonas* spp. presumably liberate nutrients from leaf tissue, as supported by their
479 own replication to populations above 10^8 CFU/cm^2 (21) and increased electrolyte leakage of

480 tomato leaf tissue (15). One hypothesis is that an infected apoplast is enriched in carbohydrates,
481 and *S. enterica* metabolizes these nutrients that it can't access on its own. *S. enterica* can utilize
482 many different sugars as sole carbon sources (57), and although only 10% of *Salmonella* species
483 can metabolize sucrose (58), one of the most prevalent carbohydrates available in plant tissues
484 (51), other sugars such as glucose and fructose (59, 60) could be available to *S. enterica*. Future
485 studies will be informative in describing *avrHah1*-independent and -dependent mechanisms by
486 which *Xanthomonas* releases host nutrients and identifying resources scavenged by *S. enterica*
487 within infected leaves.

488 Overall, we have identified a common phytobacterial disease symptom of leaf pathogens,
489 water-soaking, as a mechanism by which *S. enterica* can be passively relocated to the apoplast of
490 leaves, resulting in access to protected niches including the substomatal chamber directly below
491 the initial arrival site and distal sites of the apoplast. Our results show that *avrHah1* expression
492 by *X. gardneri* influences the fate of *S. enterica,* and considering evidence that *avrHah1* is being
493 transferred between *Xanthomonas* species, gene flow within a plant pathogen complex may have
494 dire effects on the persistence of enteric human pathogens in crop plants that eventually will be
495 consumed raw. Altogether, our findings illustrate a model for how enteric bacterial human
496 pathogens are dispersed in agricultural fields via contaminated irrigation water and subsets of the
497 bacterial population can relocate from the hostile leaf surface to a habitable niche within the
498 apoplast (Fig. 7). As phytopathogen populations evolve and respond to global environmental
499 changes, understanding their effects on the redistribution and survival of other plant-associated
500 microbes will be critical.

501 **REFERENCES**

502 1. Beattie GA. 2011. Water Relations in the Interaction of Foliar Bacterial Pathogens with
503 Plants. Annu Rev Phytopathol 49:533–555.
504 2. Schonherr J. 2006. Characterization of aqueous pores in plant cuticles and permeation of
505 ionic solutes. J Exp Bot 57:2471–2491.
506 3. Monier J, Lindow SE. 2004. Frequency , Size , and Localization of Bacterial Aggregates
507 on Bean Leaf Surfaces. Appl Environ Microbiol 70:346–355.
508 4. Barak JD, Kramer LC, Hao L-Y. 2011. Colonization of Tomato Plants by Salmonella
509 enterica Is Cultivar Dependent, and Type 1 Trichomes Are Preferred Colonization Sites.
510 Appl Environ Microbiol 77:498–504.
511 5. Xin XF, Nomura K, Aung K, Velásquez AC, Yao J, Boutrot F, Chang JH, Zipfel C, He
512 SY. 2016. Bacteria establish an aqueous living space in plants crucial for virulence.
513 Nature 539:524–529.
514 6. Schwartz AR, Morbitzer R, Lahaye T, Staskawicz BJ. 2017. TALE-induced bHLH
515 transcription factors that activate a pectate lyase contribute to water soaking in bacterial
516 spot of tomato. Proc Natl Acad Sci 114:E897–E903.
517 7. Roper MC, Burbank LP, Williams K, Viravathana P, Tien H-Y, von Bodman S. 2015. A
518 Large Repetitive RTX-Like Protein Mediates Water-Soaked Lesion Development,
519 Leakage of Plant Cell Content and Host Colonization in the Pantoea stewartii subsp.
520 stewartii Pathosystem. Mol Plant-Microbe Interact 28:1374–1382.
521 8. Goode MJ, Sasser M. 1980. Prevention - the Key to Controlling Bacterial Spot and
522 Bacterial Speck of Tomato. Plant Dis 64:831–834.
523 9. Ginnan NA, Dang T, Bodaghi S, Ruegger PM, McCollum G, England G, Vidalakis G,

524 Borneman J, Rolshausen PE, Caroline Roper M. 2020. Disease-induced microbial shifts in
525 citrus indicate microbiome-derived responses to huanglongbing across the disease severity
526 spectrum. Phytobiomes J 4:375–387.
527 10. Gao M, Xiong C, Gao C, Tsui CKM, Wang MM, Zhou X, Zhang AM, Cai L. 2021.
528 Disease-induced changes in plant microbiome assembly and functional adaptation.
529 Microbiome 9:1–18.
530 11. Yang F, Zhang J, Zhang H, Ji G, Zeng L, Li Y, Yu C, Fernando WGD, Chen W. 2020.
531 Bacterial Blight Induced Shifts in Endophytic Microbiome of Rice Leaves and the
532 Enrichment of Specific Bacterial Strains With Pathogen Antagonism. Front Plant Sci
533 11:1–14.
534 12. Teplitski M, Barak JD, Schneider KR. 2009. Human enteric pathogens in produce : un-
535 answered ecological questions with direct implications for food safety. Curr Opin
536 Biotechnol 20:166–171.
537 13. Abbott DW, Boraston AB. 2008. Structural Biology of Pectin Degradation by
538 Enterobacteriaceae. Microbiol Mol Biol Rev 72:301–316.
539 14. Islam M, Morgan J, Doyle MP, Phatak SC, Millner P, Jiang X. 2004. Fate of Salmonella
540 enterica Serovar Typhimurium on Carrots and Radishes Grown in Fields Treated with
541 Contaminated Manure Composts or Irrigation Water. Appl Environ Microbiol 70:2497–
542 2502.
543 15. Potnis N, Colee J, Jones JB, Barak JD. 2015. Plant Pathogen-Induced Water-Soaking
544 Promotes Salmonella enterica Growth on Tomato Leaves. Appl Environ Microbiol
545 81:8126–8134.
546 16. Potnis N, Soto-Arias JP, Cowles KN, van Bruggen AHC, Jones JB, Barak JD. 2014.

547 Xanthomonas perforans Colonization Influences Salmonella enterica in the Tomato
548 Phyllosphere. Appl Environ Microbiol 80:3173–3180.
549 17. Kwan G, Charkowski AO, Barak JD. 2013. Salmonella enterica Suppresses
550 Pectobacterium carotovorum subsp. carotovorum Population and Soft Rot Progression by
551 Acidifying the Microaerophilic Environment. MBio 4:1–9.
552 18. Cowles KN, Groves RL, Barak JD. 2018. Leafhopper-Induced Activation of the Jasmonic
553 Acid Response Benefits Salmonella enterica in a Flagellum-Dependent Manner. Front
554 Microbiol 9:1–15.
555 19. Harrod VL, Groves RL, Maurice MA, Barak JD. 2021. Frankliniella occidentalis facilitate
556 Salmonella enterica survival in the phyllosphere. PLoS One 16:1–16.
557 20. Wells JM, Butterfield JE. 1997. Salmonella contamination associated with bacterial soft
558 rot of fresh fruits and vegetables in the marketplace. Plant Dis 81:867–872.
559 21. Cowles KN, Block AK, Barak JD. Xanthomonas hortorum pv. gardneri TAL effector
560 AvrHah1 is neessary and sufficient for increased persistence of Salmonella enterica on
561 tomato leaves. Res Sq https://doi.org/10.21203/rs.3.rs-1229600/v1.
562 22. Hoagland L, Ximenes E, Ku S, Ladisch M. 2018. Foodborne pathogens in horticultural
563 production systems : Ecology and mitigation. Sci Hortic (Amsterdam) 236:192–206.
564 23. Centers for Disease Control and Prevention (CDC). 2008. Outbreak of Salmonella
565 Serotype Saintpaul Infections Associated with Multiple Raw Produce Items --- United
566 States, 2008. Morb Mortal Wkly Rep 57:929–934.
567 24. Centers for Disease Control and Prevention (CDC). 2018. Multistate Outbreak of E. coli
568 O157:H7 Infections Linked to Romaine Lettuce (Final Update).
569 25. Kroupitski Y, Golberg D, Belausov E, Pinto R, Swartzberg D, Granot D, Sela S. 2009.

570 Internalization of Salmonella enterica in Leaves Is Induced by Light and Involves
571 Chemotaxis and Penetration through Open Stomata †. Appl Environ Microbiol
572 75:6076–6086.
573 26. Golberg D, Kroupitski Y, Belausov E, Pinto R, Sela S. 2011. Salmonella Typhimurium
574 internalization is variable in leafy vegetables and fresh herbs. Int J Food Microbiol
575 145:250–257.
576 27. Chahar M, Kroupitski Y, Gollop R, Belausov E, Melotto M, Sela-Saldinger S. 2021.
577 Determination of Salmonella enterica Leaf Internalization Varies Substantially According
578 to the Method and Conditions Used to Assess Bacterial Localization. Front Microbiol
579 12:1–12.
580 28. Schornack S, Minsavage G V, Stall RE, Jones JB, Lahaye T, Jones JB. 2006.
581 Characterization of AvrHah1 , a novel AvrBs3-like effector from Xanthomonas gardneri
582 with virulence and avirulence activity. New Phytol 179:546–556.
583 29. Collmer A, Keen NK. 1986. The Role of Pectic Enzymes in Plant Pathogenesis. Annu Rev
584 Phytopathol 24:383–409.
585 30. Clayton E. 1936. Water-Soaking of leaves in relation to development of the wildfire
586 disease of tobacco. J Agric Res 52:239–269.
587 31. Sommers CH, Sites JE, Musgrove M. 2010. Ultraviolet light (254 nm) inactivation of
588 pathogens on foods and stainless steel surfaces. J Food Saf 30:470–479.
589 32. Wilson M, Hirano SS, Lindow SE. 1999. Location and survival of leaf-associated bacteria
590 in relation to pathogenicity and potential for growth within the leaf. Appl Environ
591 Microbiol 65:1435–1443.
592 33. Kennedy BW, Ercolani GL. 1978. Soybean Primary Leaves as a Site for Epiphytic

593 Multiplication of Pseudomonas glycinea. Ecol Epidemiol 68:1196–1201.
594 34. Döhring T. 2017. Critical discussion on the UV absorption properties of Earth's
595 atmosphere.Proceedings of SPIE 10453.
596 35. Vogelmann TC, Bjorn LO. 1986. Plants as light traps. Physiol Plantarium 68:704–708.
597 36. Doan HK, Ngassam VN, Gilmore SF, Tecon R, Parikh AN, Leveau JHJ. 2020.
598 Topography-driven shape, spread, and retention of leaf surface water impacts microbial
599 dispersion and activity in the phyllosphere. Phytobiomes J 4:268–280.
600 37. Fino VR, Kniel KE. 2008. UV light inactivation of hepatitis A virus, aichi virus, and
601 feline calicivirus on strawberries, green onions, and lettuce. J Food Prot 71:908–913.
602 38. Huang R, Chen H. 2019. Comparison of Water-Assisted Decontamination Systems of
603 Pulsed Light and Ultraviolet for Salmonella Inactivation on Blueberry, Tomato, and
604 Lettuce. J Food Sci 84:1145–1150.
605 39. Schonherr J. 1972. Penetration of Stomata by Liquids 813–819.
606 40. Haefele DM, Lindow SE. 1987. Flagellar Motility Confers Epiphytic Fitness Advantages
607 Pseudomonas syringae. Appl Environ Microbiol 53:2528–2533.
608 41. Rufian J, Sanchez-Romero M, Lopez-Marquez D, Macho A, Mansfield J, Arnold D, Ruiz-
609 Albert J, Casadesus J, Beuzon C. 2016. Pseudomonas syringae differentiates into
610 phenotypically distinct subpopulations during colonization of a plant host. Environ
611 Microbiol 18:3593–3605.
612 42. Sahin F, Miller SA. 1997. Identification of the bacterial leaf spot pathogen of lettuce,
613 Xanthomonas campestris pv. vitians, in Ohio, and assessment of cultivar resistance and
614 seed treatment. Plant Dis 81:1443–1446.
615 43. Dia NC, Morinière L, Cottyn B, Bernal E, Jacobs JM, Koebnik R, Osdaghi E, Potnis N,

616 Pothier JF. 2022. Xanthomonas hortorum – beyond gardens: Current taxonomy,
617 genomics, and virulence repertoires . Mol Plant Pathol 1–25.
618 44. Potnis N, Krasileva K, Chow V, Almeida NF, Patil PB, Ryan RP, Sharlach M, Behlau F,
619 Dow JM, Momol MT, White FF, Preston JF, Vinatzer BA, Koebnik R, Setubal JC,
620 Norman DJ, Staskawicz BJ, Jones JB. 2011. Comparative genomics reveals diversity
621 among xanthomonads infecting tomato and pepper. BMC Genomics 12:1–23.
622 45. Schwartz AR, Potnis N, Timilsina S, Wilson M, Patane J, Martins J, Minsavage G V.,
623 Dahlbeck D, Akhunova A, Almeida N, Vallad GE, Barak JD, White FF, Miller SA,
624 Ritchie D, Goss E, Bart RS, Setubal JC, Jones JB, Staskawicz BJ. 2015. Phylogenomics of
625 Xanthomonas field strains infecting pepper and tomato reveals diversity in effector
626 repertoires and identifies determinants of host specificity. Front Microbiol 6:1–17.
627 46. Newberry EA, Bhandari R, Minsavage G V., Timilsina S, Jibrin MO, Kemble J, Sikora
628 EJ, Jones JB, Potnis N. 2019. Independent Evolution with the Gene Flux Originating from
629 Multiple Xanthomonas Species Explains Genomic Heterogeneity in Xanthomonas
630 perforans. Appl Environ Microbiol 85:1–17.
631 47. Beattie GA, Lindow SE. 1995. The secret life of foliar bacterial pathogens on leaves.
632 Annu Rev Phytopathol 33:145–172.
633 48. Pfeilmeier S, Caly DL, Malone JG. 2016. Bacterial pathogenesis of plants: future
634 challenges from a microbial perspective. Mol Plant Pathol 7:1298–1313.
635 49. Monier J, Lindow SE. 2003. Pseudomonas syringae Responds to the Environment on
636 Leaves by Cell Size Reduction 93:1209–1216.
637 50. Leveau JHJ, Lindow SE. 2001. Appetite of an epiphyte: Quantitative monitoring of
638 bacterial sugar consumption in the phyllosphere. Proc Natl Acad Sci 98:3446–3453.

639 51. Fatima U, Senthil-Kumar M. 2015. Plant and pathogen nutrient acquisition strategies.
640 Front Plant Sci 6:1–12.
641 52. Ferelli AMC, Bolten S, Szczesny B, Micallef SA. 2020. Salmonella enterica Elicits and Is
642 Restricted by Nitric Oxide and Reactive Oxygen Species on Tomato. Front Microbiol
643 11:1–15.
644 53. Meng F, Altier C, Martin GB. 2013. Salmonella colonization activates the plant immune
645 system and benefits from association with plant pathogenic bacteria. Environ Microbiol
646 15:2418–2430.
647 54. Garcia AV, Charrier A, Schikora A, Bigeard J, Pateyron S, de Tauzia-moreau M-L,
648 Evrard A, Mithöfer A, Martin-magniette ML, Virlogeux-Payant I, Hirt H. 2014.
649 Salmonella enterica Flagellin Is Recognized via FLS2 and Activates PAMP-Triggered
650 Immunity in Arabidopsis thaliana. Mol Plant 7:657–674.
651 55. Wahlig TA, Bixler BJ, Valdés-López O, Mysore KS, Wen J, Ané JM, Kaspar CW. 2019.
652 Salmonella enterica serovar Typhimurium ATCC 14028S is tolerant to plant defenses
653 triggered by the flagellin receptor FLS2. FEMS Microbiol Lett 366:1–7.
654 56. Roy D, Panchal S, Rosa BA, Melotto M. 2013. Escherichia coli O157:H7 Induces
655 Stronger Plant Immunity than Salmonella enterica Typhimurium SL1344. Phytopathology
656 103:326–332.
657 57. Tracy BS, Edwards KK, Eisenstark A. 2002. Carbon and nitrogen substrate utilization by
658 archival Salmonella typhimurium LT2 cells. BMC Evol Biol 2:1–6.
659 58. Reid SJ, Abratt VR. 2005. Sucrose utilisation in bacteria: Genetic organisation and
660 regulation. Appl Microbiol Biotechnol 67:312–321.
661 59. O'Leary BM, Neale HC, Geilfus CM, Jackson RW, Arnold DL, Preston GM. 2016. Early

662 changes in apoplast composition associated with defence and disease in interactions
663 between Phaseolus vulgaris and the halo blight pathogen Pseudomonas syringae Pv.
664 phaseolicola. Plant Cell Environ 39:2172–2184.
665 60. Courbier S, Grevink S, Sluijs E, Bonhomme PO, Kajala K, Van Wees SCM, Pierik R.
666 2020. Far-red light promotes Botrytis cinerea disease development in tomato leaves via
667 jasmonate-dependent modulation of soluble sugars. Plant Cell Environ 43:2769–2781.
668

669 **ACKNOWLEDGEMENTS**

670 This material is based upon work supported by the National Science Foundation Graduate
671 Research Fellowship under Grant No. DGE-1747503 and by USDA-HATCH grant no.
672 WIS03022. Any opinions, findings, and conclusions or recommendations expressed in this
673 material are those of the author(s) and do not necessarily reflect the views of the National
674 Science Foundation. The funders had no role in study design, data collection, and interpretation,
675 or the decision to submit the work for publication.
676

677 We are grateful to J. Jones and G. Minsavage for providing the *Xanthomonas gardneri*
678 Δ*avrHah1* strain used in this work. Additionally, we thank C. Solís-Lemus and N. Keuler for
679 providing guidance on statistical analysis.
680

681 Author Contributions: MHD, KNC, and JDB developed the experiments. MHD, KNC, SCZ, and
682 INM performed the experiments. MHD and JDB wrote the manuscript, and all authors reviewed
683 the manuscript. MHD created the original illustrations.
684

687 **TABLES**

688 Table 1: Bacterial strains used in this study.

Strain Abbreviation	Description	Reference or Source
Xg WT	*Xanthomonas hortorum* pv. *gardneri* 444; Nal^R	(21)
Xg avr-	*Xanthomonas hortorum* pv. *gardneri* 444; *avrHah1*$^{\Delta DBD}$	received from J. Jones; (21)
Xv	*Xanthomonas vesicatoria* 1111; Nal^R	ATCC
Se WT	*Salmonella enterica* sv. Typhimurium 14028s; Kan^R	(21)
Se Δ*motA*	*Salmonella enterica* sv. Typhimurium 14028s; Δ*motA*::Kan	(18)

689

690 **Figure Legend**

691 Figure 1: Infiltration and droplet inoculation assay. (A) Tomato leaflets were infiltrated with
692 water or bacteria through the abaxial surface; infiltration zones are indicated with a thick black
693 line and darker green shading. (B) Droplets of *S. enterica* (*Se*) cell suspension were then applied
694 to the adaxial surface of each infiltration zone at a site marked with permanent marker,
695 represented by black dash marks. The *Se* arrival day occurred 0-2 days post-infiltration (DPI).
696 (C) When the *Se* cells arrived on the plant via droplet application, several apoplast states were
697 possible depending on the infiltration treatment received. Circle symbols (healthy: open circle,
698 infected: bacteria-filled circle; dry: white circle, wet: turquoise circle) depict the various apoplast
699 states in subsequent data figures. (D) Designated leaflets were detached and irradiated with UV
700 at indicated timepoints, which ranged from 2.5 hours post-*Se* arrival (HPA) to 3 days post-Se
701 arrival (DPA) depending on the experiment. Tissue was sampled immediately after UV
702 irradiation at the site of *S. enterica* arrival (blue dotted circle) and non-overlapping distal tissue
703 (yellow dotted circles) for *Se* population enumeration.

704 Figure 2: Healthy leaf tissue with a water-filled apoplast facilitates localization to a protected
705 niche and migration to distal tissue. *S. enterica* (*Se*) was applied by droplet (10^6 CFU/leaflet) at 2
706 or 0 days post-infiltration (DPI) with water (blue boxplots). Half of leaflets were UV-irradiated
707 (triangle points; light-shaded boxplots) and the other half were left non-irradiated (circle points;
708 dark-shaded boxplots). *Se* populations were sampled at 1 day post *Se*-arrival (DPA) at the droplet
709 arrival site and distal from the arrival site. *Se* populations from droplet-inoculated leaflets were
710 compared to those from control leaflets infiltrated with *S. enterica* (gray boxplots). Uppercase
711 letters above the boxplots denote significance among treatment groups within the arrival site
712 based on an ANOVA and post-hoc Tukey test ($P < 0.05$). Lowercase letters denote significance
713 among treatment groups within the distal site based on a Kruskal-Wallis and post-hoc Wilcox
714 test ($P < 0.05$). Dotted line indicates limit of detection. Refer to Figure 1, panel C for circle
715 symbol key describing apoplast states.
716 Figure 3: *X. gardneri* infection facilitates *S. enterica* localization to protected niche and
717 migration beyond site of arrival. *S. enterica* (*Se*) was applied by droplet (10^6 CFU/leaflet) at 0
718 days post-infiltration (DPI) with water (blue boxplots) or 2 DPI with *X. gardneri* (*Xg* WT;
719 orange boxplots). Half of leaflets were UV-irradiated (triangle points; light-shaded boxplots) and
720 the other half were left non-irradiated (circle points; dark-shaded boxplots). *Se* populations were
721 sampled at 1 day post *Se*-arrival (DPA) at the droplet arrival site and distal from the arrival site
722 (distal site for *Xg*). Uppercase letters above the boxplots denote significance among treatment
723 groups within the arrival site based on an ANOVA and post-hoc Tukey test ($P < 0.05$).
724 Lowercase letters denote significance among treatment groups within the distal site based on a
725 Kruskal-Wallis and post-hoc Wilcox test ($P < 0.05$). Dotted line indicates limit of detection.
726 Refer to Figure 1, panel C for circle symbol key describing apoplast states.

727 Figure 4: *S. enterica* access to protected niche within 2.5 hours of arrival on water-soaked tissue
728 depends on *Xanthomonas* strain and duration of infection. *S. enterica* (*Se*) was applied by droplet
729 (10^6 CFU/leaflet) to leaflets infiltrated with water (blue boxplots), *X. gardneri* WT (*Xg* WT;
730 orange boxplots), *X. gardneri avrHah1*$^{\Delta DBD}$ (*Xg avr;* pink boxplots), or *X. vesicatoria* (*Xv*; green
731 boxplots) at indicated days post-infiltration (DPI). (A) Unabsorbed *S. enterica* (*Se*) droplet
732 volumes measured 2.5 hours following droplet application. Differing letters above the plot
733 denote significantly different treatment groups based on a Kruskal-Wallis and post-hoc Wilcox
734 multiple comparison test ($P < 0.05$). (B) Reduction of *S. enterica* populations in response to UV
735 irradiation at the *Se* droplet arrival site at 2.5 hours-post *Se* arrival (HPA). Letters above the
736 boxplots denote significance among treatment groups based on an ANOVA and post-hoc Tukey
737 test ($P < 0.05$). Refer to Figure 1, panel C for circle symbol key describing apoplast states.
738 Figure 5: *X. gardneri avrHah1* enhances *S. enterica* migration during early infection, and
739 flagellar motility promotes *S. enterica* survival at distal tissue. *S. enterica* (*Se*) WT (circle points)
740 or Δ*motA* (asterisk points) was applied by droplet (10^6 CFU/leaflet) at 1 or 2 days post-
741 infiltration (DPI) with *X. gardneri* WT (*Xg* WT, orange boxplots) or *X. gardneri avrHah1*$^{\Delta DBD}$
742 (*Xg avr*; pink boxplots). *Se* populations were sampled at 1 day post *Se*-arrival (DPA) distal from
743 the *Se* droplet arrival site without UV irradiation treatment. Letters above the boxplots denote
744 significance among treatment groups based on a Kruskal-Wallis and post-hoc Wilcox test ($P <$
745 0.05). Dotted line indicates limit of detection. Refer to Figure 1, panel C for circle symbol key
746 describing apoplast states.
747 Figure 6: *Xanthomonas*-infected apoplast serves as a hospitable niche for *S. enterica* 3 days post-
748 arrival. *S. enterica* (*Se*) was applied by droplet (10^6 CFU/leaflet) to leaflets infiltrated with water
749 (blue boxplots), *X. gardneri* WT (*Xg* WT; orange boxplots), *X. gardneri avrHah1*$^{\Delta DBD}$ (*Xg avr;*

750 pink boxplots), or *X. vesicatoria* (*Xv*; green boxplots) at indicated days post-infiltration (DPI). *Se*
751 populations were sampled at 3 days post *Se*-arrival (DPA) from the arrival site and distal from
752 the arrival site. All leaflets were UV irradiated prior to sampling. Uppercase letters above the
753 boxplots denote significance among treatment groups within the arrival site based on an
754 ANOVA and post-hoc Tukey test ($P < 0.05$). Lowercase letters denote significance among
755 treatment groups within the distal site based on a Kruskal-Wallis and post-hoc Wilcox test ($P <$
756 0.05). Dotted line indicates limit of detection. Refer to Figure 1, panel C for circle symbol key
757 describing apoplast states.
758 Figure 7: *X. gardneri*-infected apoplast enables replication of *S. enterica* within protected niches.
759 *S. enterica* (*Se*) was applied by droplet (10^3 CFU/leaflet) to leaflets infiltrated with water (blue
760 boxplots), *X. gardneri* WT (*Xg* WT; orange boxplots), *X. gardneri avrHah1*$^{\Delta DBD}$ (*Xg avr;* pink
761 boxplots), or *X. vesicatoria* (*Xv*; green boxplots) at indicated days post-infiltration (DPI). *Se*
762 populations were destructively sampled at 2.5 hours post *Se*-arrival (HPA) and 3 days post *Se*-
763 arrival (DPA) at the droplet arrival site and distal from the arrival site. All leaflets were UV
764 irradiated prior to sampling. Letters above the boxplots denote significance between the
765 healthy/wet (H2O 0 DPI) and Xg treatment groups within the arrival (uppercase) and distal
766 (lowercase) sites based on an ANOVA and post-hoc Tukey test ($P < 0.05$). Dotted line indicates
767 limit of detection (LOD). Zero values were confirmed via LB enrichment. Points plotted at
768 LOD/2 indicate absence of colonies via direct plating and a positive enrichment sample. Refer to
769 Figure 1, panel C for circle symbol key describing apoplast states.
770 Figure 8: Model for *S. enterica* survival in a habitable apoplast. *S. enterica* can colonize crop
771 plants via spray-irrigation of contaminated water. Macroscopically dry tissue (a) does not enable
772 absorption of surface water, whereas tissue with an aqueous apoplast (b) facilitates the ingression

773 of *S. enterica* into the apoplast. Healthy tissue that is abiotically water-soaked eventually dries
774 out (c), creating an unfavorable niche for *S. enterica.* By contrast, an infected apoplast (d), which
775 maintains water-soaking via phytopathogen effectors and is likely enriched with nutrients and
776 other growth-promoting factors, facilitates *S. enterica* replication.

FIGURE 1

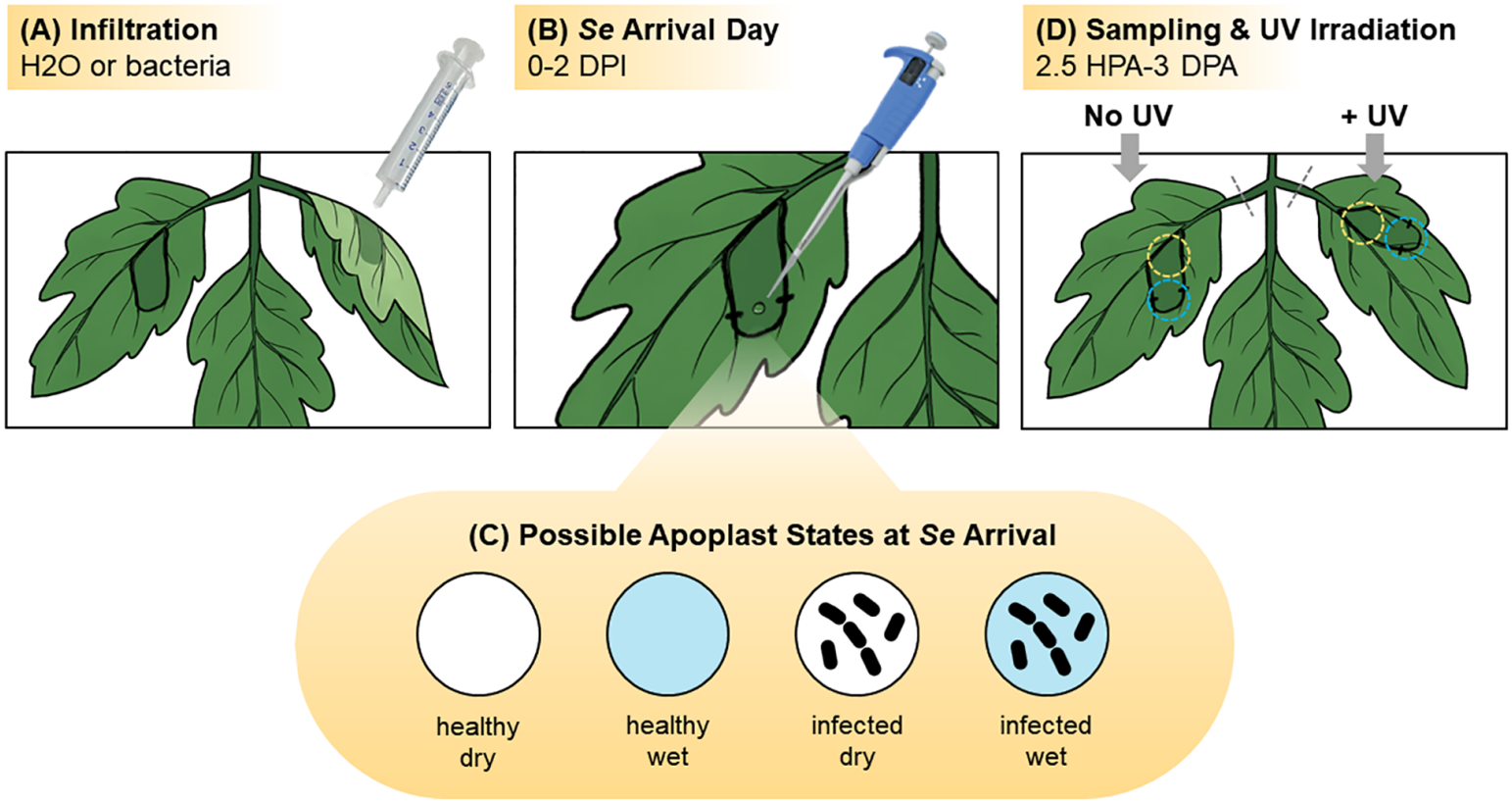
(A) Infiltration
H2O or bacteria
(B) Se Arrival Day
0-2 DPI
(D) Sampling & UV Irradiation
2.5 HPA-3 DPA
No UV
+ UV
(C) Possible Apoplast States at Se Arrival
healthy dry
healthy wet
infected dry
infected wet

FIGURE 2

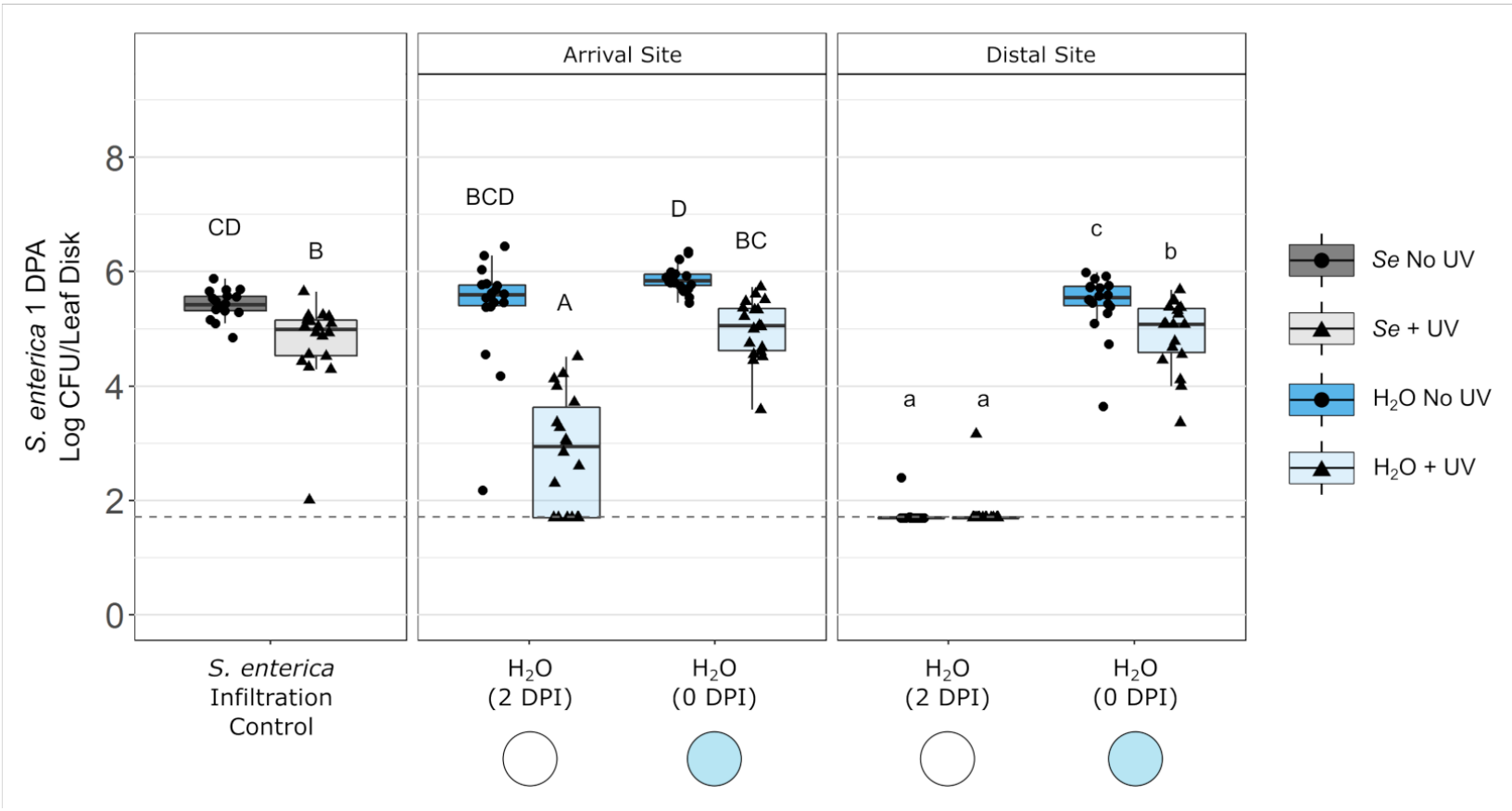
Arrival Site
Distal Site
S. enterica 1 DPA
Log CFU/Leaf Disk
8
6
4
2
0
CD
B
BCD
A
D
BC
a
a
c
b
S. enterica
Infiltration
Control
H2O
(2 DPI)
H2O
(0 DPI)
H2O
(2 DPI)
H2O
(0 DPI)
Se No UV
Se + UV
H2O No UV
H2O + UV

FIGURE 3

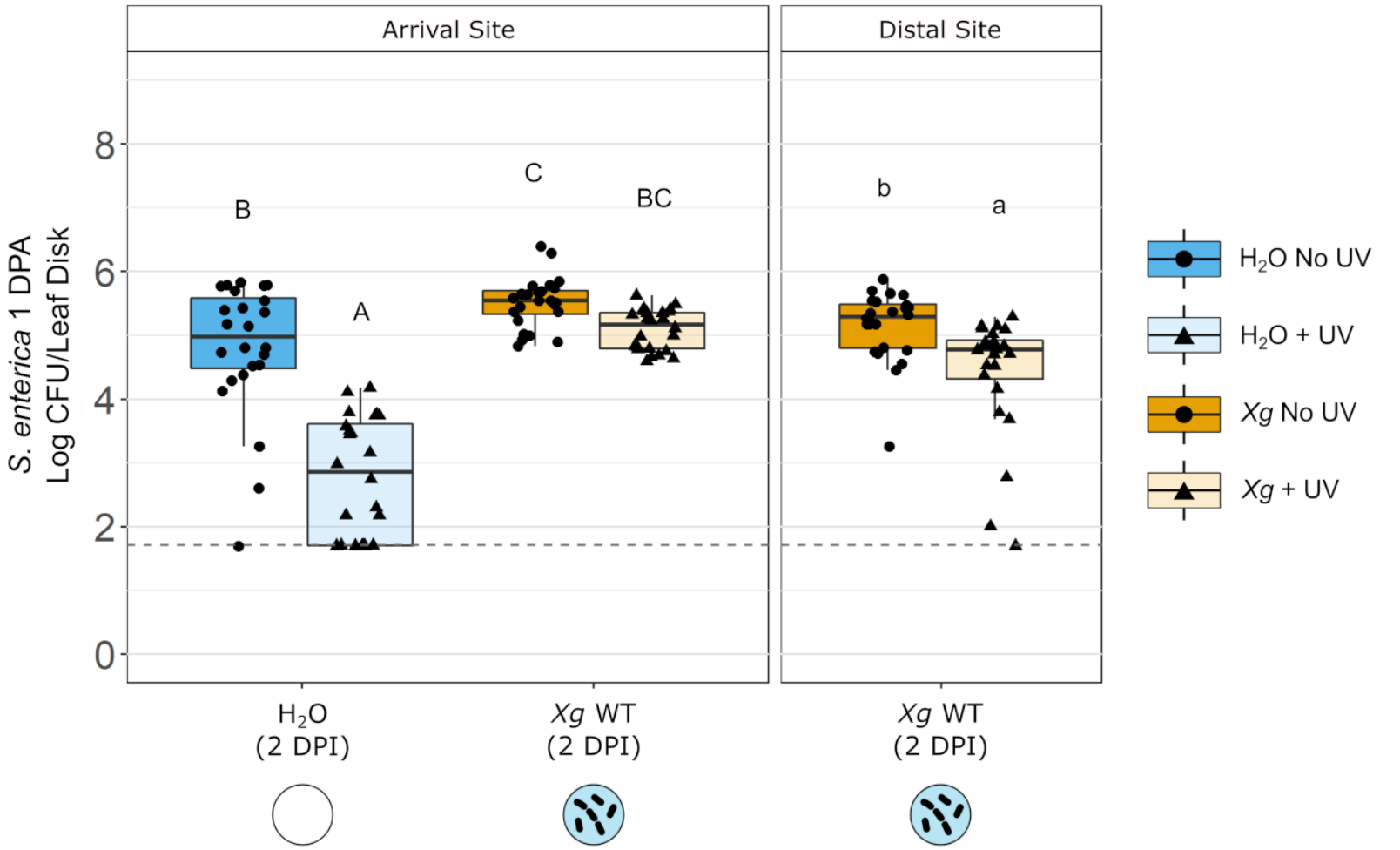
Arrival Site
Distal Site
S. enterica 1 DPA
Log CFU/Leaf Disk
8
6
4
2
0
B
A
C
BC
b
a
H2O
(2 DPI)
Xg WT
(2 DPI)
Xg WT
(2 DPI)
H2O No UV
H2O + UV
Xg No UV
Xg + UV

FIGURE 4

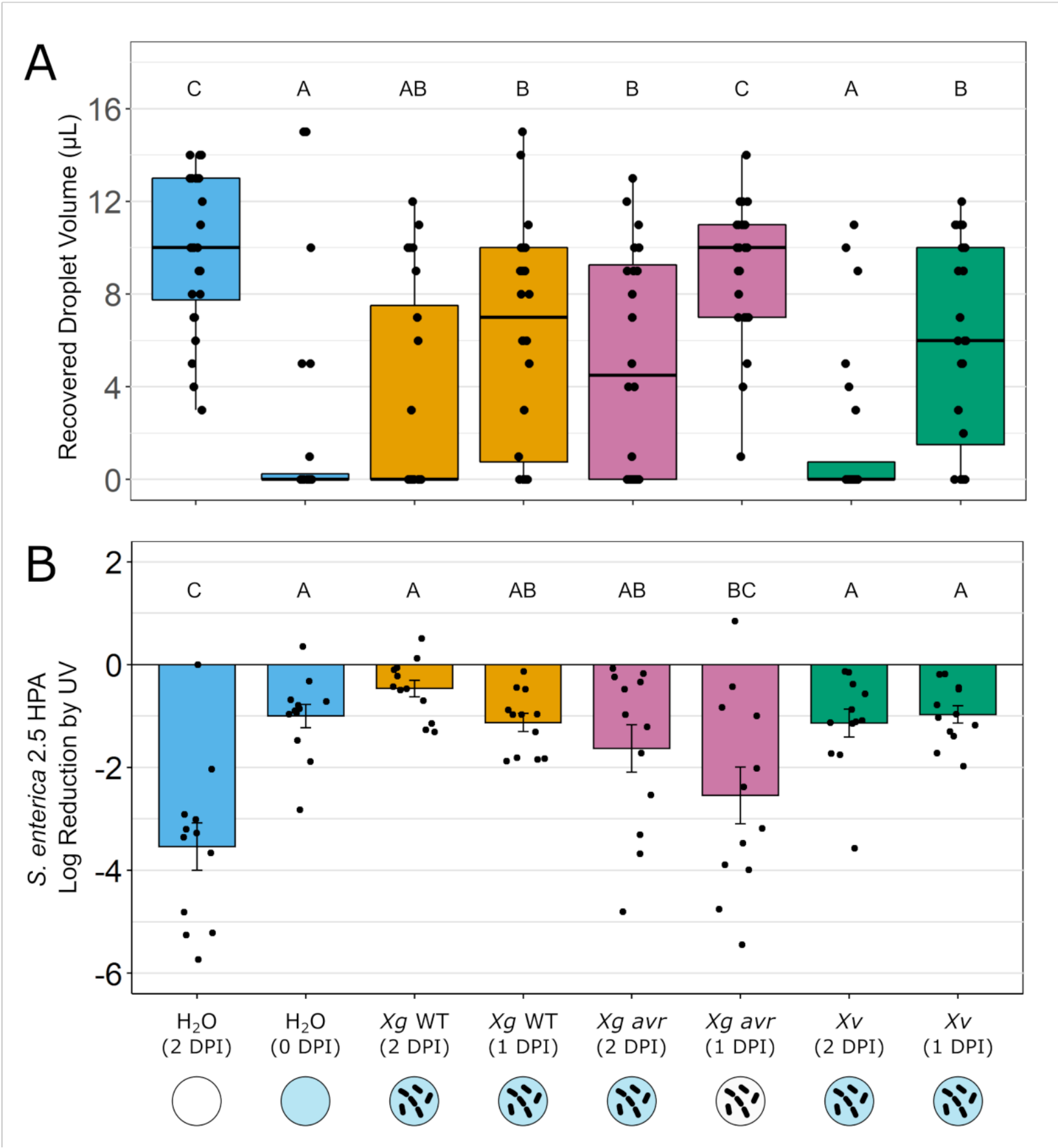
A
Recovered Droplet Volume (µL)
16
12
8
4
0
C
A
AB
B
B
C
A
B
B
S. enterica 2.5 HPA
Log Reduction by UV
2
0
-2
-4
-6
C
A
A
AB
AB
BC
A
A
H2O (2 DPI)
H2O (0 DPI)
Xg WT (2 DPI)
Xg WT (1 DPI)
Xg avr (2 DPI)
Xg avr (1 DPI)
Xv (2 DPI)
Xv (1 DPI)

FIGURE 5

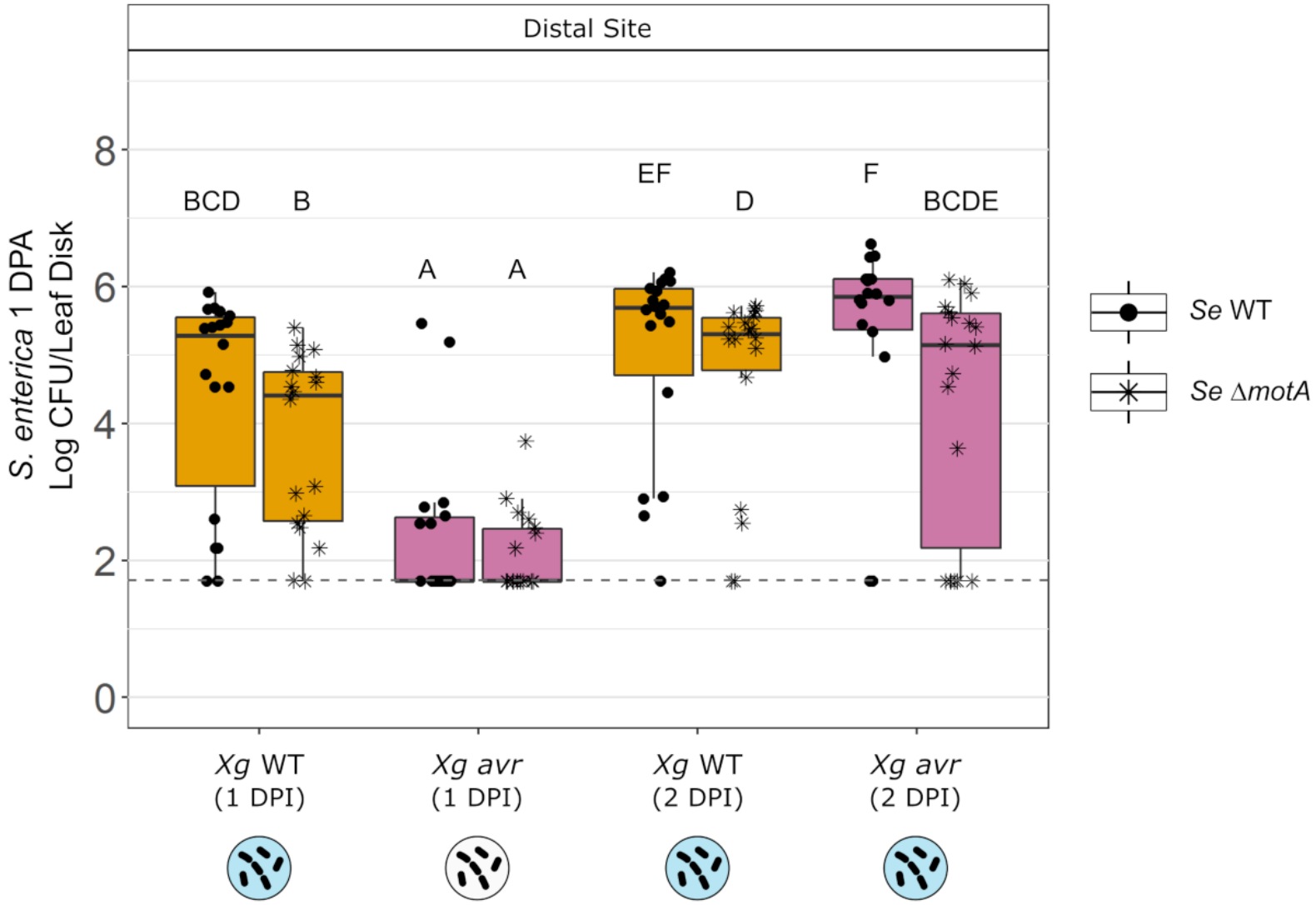
Distal Site
S. enterica 1 DPA
Log CFU/Leaf Disk
8
6
4
2
0
BCD
B
A
A
EF
D
F
BCDE
Xg WT
(1 DPI)
Xg avr
(1 DPI)
Xg WT
(2 DPI)
Xg avr
(2 DPI)
Se WT
Se ΔmotA

FIGURE 6

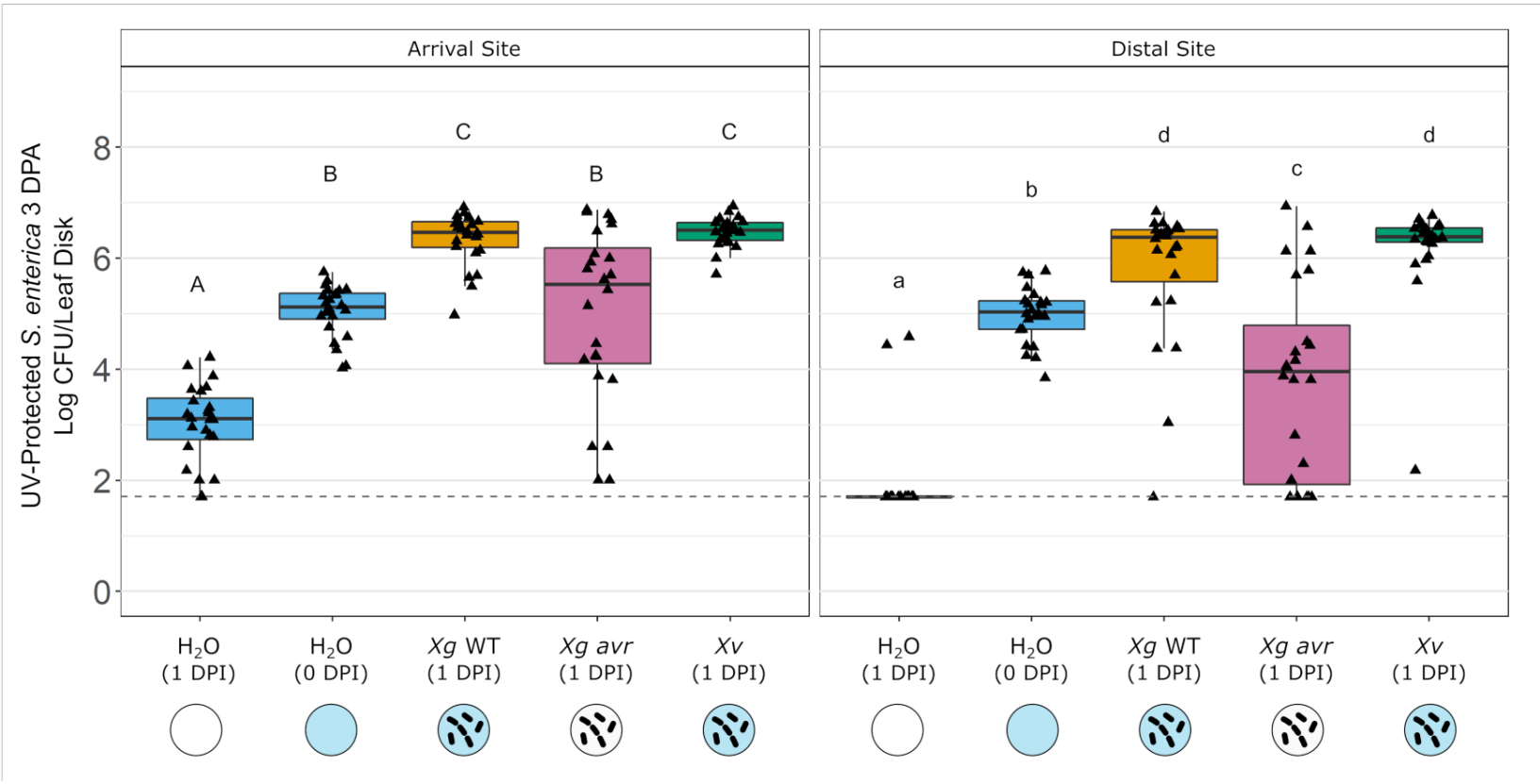
Arrival Site
Distal Site
UV-Protected S. enterica 3 DPA
Log CFU/Leaf Disk
0
2
4
6
8
A
B
C
B
C
a
b
d
c
d
H2O (1 DPI)
H2O (0 DPI)
Xg WT (1 DPI)
Xg avr (1 DPI)
Xv (1 DPI)

FIGURE 7

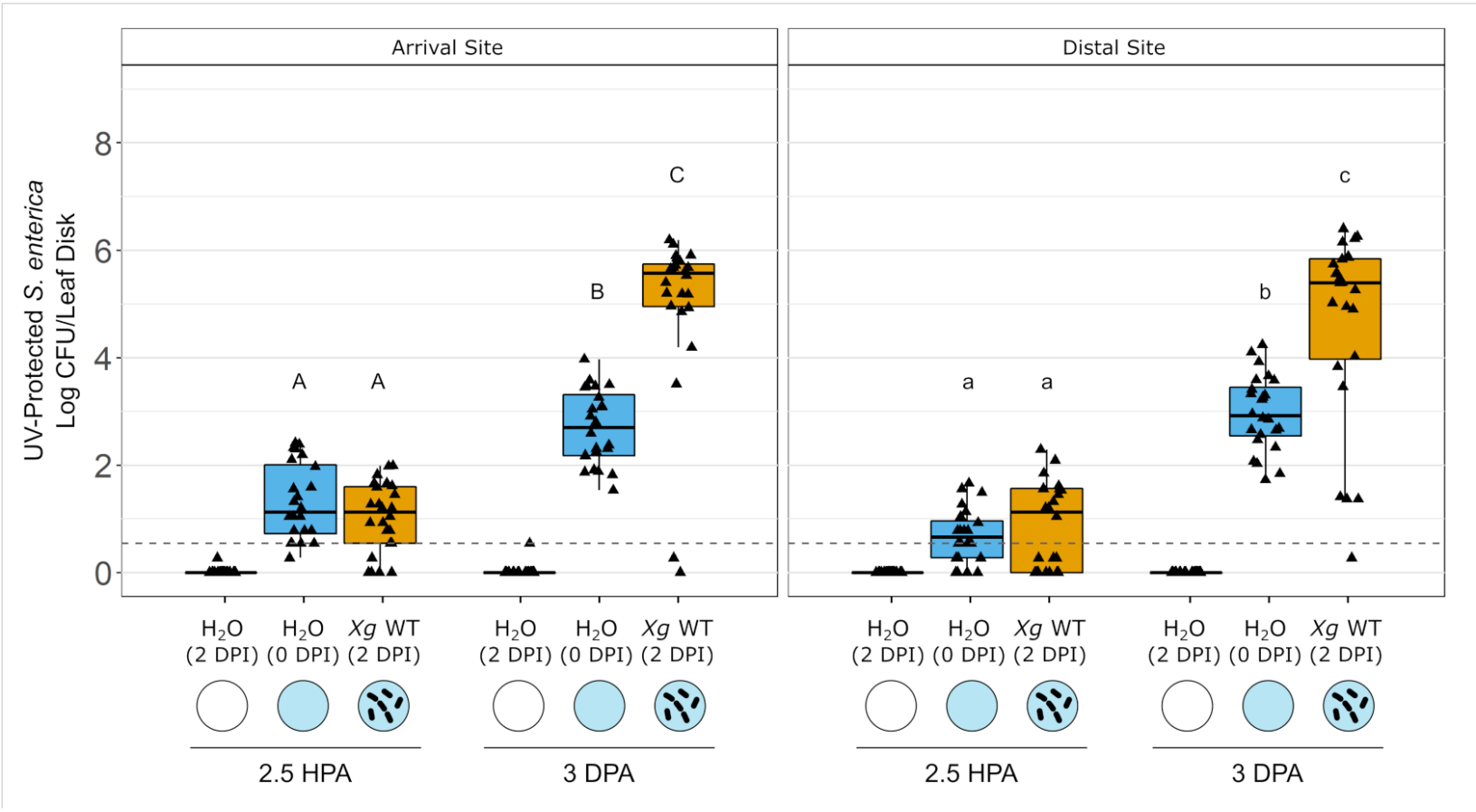
Arrival Site
Distal Site
UV-Protected S. enterica
Log CFU/Leaf Disk
8
6
4
2
0
A
A
B
C
a
a
b
c
H2O (2 DPI)
H2O (0 DPI)
Xg WT (2 DPI)
2.5 HPA
3 DPA
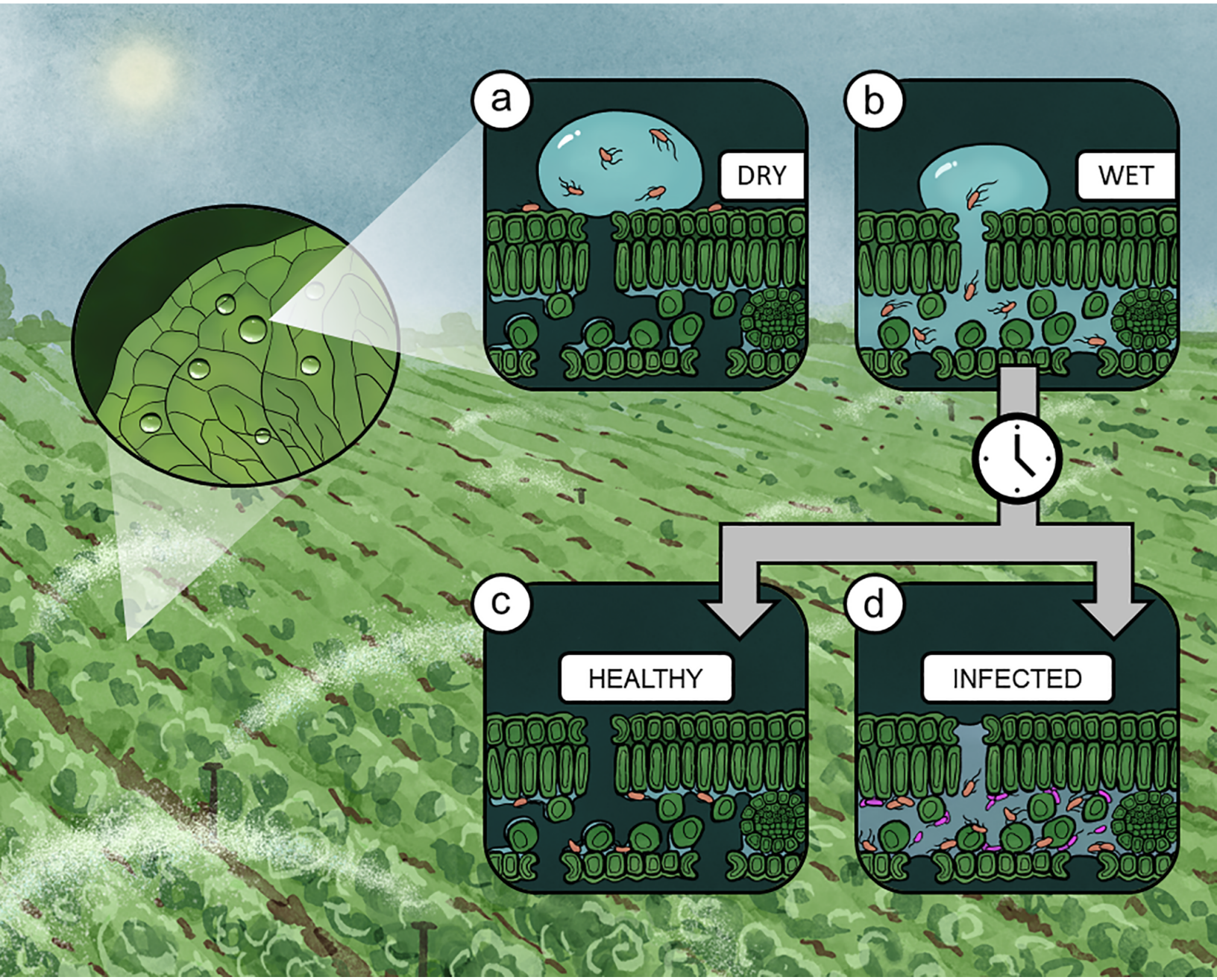
FIGURE 8